Characterization of heterogeneity and dynamics of lysis of single *Bacillus subtilis* cells upon prophage induction during spore germination and outgrowth, and vegetative growth, using Raman tweezers and live-cell imaging

Mei-yan Wu[1,2], Wen-wei Li[1], Graham Christie[3], Peter Setlow[4] and Yong-qing Li[2,5*]

[1]The laboratory for Biomedical Photonics & Engineering and School of Basic Medical Sciences, Guangxi Medical University, Nanning, Guangxi 530021, P. R. China;

[2]Department of Physics, East Carolina University, Greenville, North Carolina 27858-4353, USA;

[3]Department of Chemical Engineering and Biotechnology, University of Cambridge, Cambridge CB3 0AS, UK;

[4]Department of Molecular Biology and Biophysics, UCONN Health, Farmington, Connecticut 06030-3305, USA;

[5]School of Electronic Engineering, Dongguan University of Technology, Dongguan, Guangdong 523808, P.R. China

*Address correspondence to Yong-qing Li, East Carolina University, Department of Physics, Greenville, North Carolina 27858-4353 United States of America; Tel: 252-328-1858; Fax: 252-328-6314; E-mail: liy@ecu.edu

ABSTRACT: A prophage comprises a bacteriophage genome that has integrated into a host bacterium's DNA and which generally permits the cell to grow and divide normally. However, the prophage can be induced by various stresses, or induction can occur spontaneously. After prophage induction, viral replication and production of endolysins begin until the cell lyses and phage are released. However, the heterogeneity of prophage induction and lysis of individual cells in a population and the dynamics of a cell undergoing lysis by prophage induction have not been fully characterized. Here, we used Raman tweezers and live-cell phase contrast microscopy to characterize the Raman spectral and cell length changes that occur during the lysis of individual *Bacillus subtilis* cells from spores that carry PBSX prophage during spores' germination, outgrowth, and then vegetative growth. Major findings of this work were: (i) after addition of xylose to trigger prophage induction, the intensities of Raman spectral bands associated with nucleic acids of single cells in induced cultures gradually fell to zero, in contrast to much smaller changes in protein band intensities, and no changes in nucleic acids bands in un-induced cultures; (ii) the nucleic acids band intensities from an individual induced cell exhibited a rapid decrease, following a long lag period; (iii) after the addition of nutrient-rich medium with xylose, single spores underwent a long period (228±41.4 min) for germination, outgrowth, and vegetative growth, followed by a short period of cell burst in 1.5±0.8 min at a cell length of 8.2±5.5 μm; (iv) the latent time (T_{latent}) between addition of xylose and the start of cell burst was heterogeneous in cell populations, however, the period (ΔT_{burst}) from the latent time to completion of cell lysis was quite small; (v) in a poor medium with L-alanine alone, addition of xylose caused prophage induction following spore germination but with longer T_{latent} and ΔT_{burst} times, and without cell elongation; (vi) spontaneous prophage induction and lysis of individual cells from spores in a minimal nutrient medium was observed without xylose addition, and cell length prior to cell lysis was ~4.1 μm, but

spontaneous prophage induction was not observed in a rich medium; (vii) in a rich medium, addition of xylose at a time well after spore germination and outgrowth significantly shortened the average T_{latent} time. The results of this study provide new insight into the heterogeneity and dynamics of lysis of individual *B. subtilis* cells derived from spores upon prophage induction.

Key words: bacterium prophage induction, Raman spectroscopy, live-cell imaging, heterogeneity and dynamics of cell lysis

1. Introduction

Bacteriophages are viruses that infect bacteria. A prophage is a latent state of a bacteriophage, where the genome is integrated into the bacterial chromosome without causing disruption to the bacterial cell [1-3]. This prophage can coexist silently with its host such that the bacterial cell continues to grow and divide normally, and the genetic material of the bacteriophage is transmitted to daughter cells at each subsequent cell division. However, when the host cell is subjected to physiological stress, such as induced by UV light, high temperature or some chemicals, the prophage can be activated in a process called prophage induction, leading to the phage lytic cycle [1, 2] in which the phage commandeers the cell's macromolecular synthesis machinery and the expression of phage genes leads to synthesis of phage mRNAs, proteins and DNA, phage particle assembly, DNA packaging and ultimately bacterial lysis [2]. The host cell may eventually be filled with new virions and then lyses or bursts so that the phage particles are released into the environment and are able to infect other bacteria [1, 2]. Some prophage in bacterial cells are also able to be spontaneously activated in the absence of an external trigger, and this spontaneous activation can also lead to phage particle production and cell lysis [4, 5].

Prophage induction and cell lysis in bacterial populations has been extensively studied for the fundamental analysis of bacteriophage-host interactions [1-3], and for the applications of phage therapy for bacterial infections [6-8], and drug delivery [9, 10]. Notably, most phage in the human gut are in a latent state and integrated into the genomes of their bacterial hosts as prophage [11]. These prophages in gut bacteria can be induced by certain foods and chemicals [8, 12]. Prophage induction in gut bacteria may result in the horizontal transfer of genes to other bacterial strains or species and can also alter the relative abundance of bacterial species/strains [8].

Generally, prophage induction and lysis of individual cells within populations has not been well studied, and questions remain concerning: i) the time span for an individual cell to initiate cell lysis after prophage induction; ii) the heterogeneity between individual cells in time of the latent phase from prophage induction to the start of cell lysis; and iii) the dynamic changes in molecular composition and cell length during prophage-induced lysis of a single cell. Detailed understanding of prophage-induced cell lysis at the single-cell level and heterogeneity among a population of cells is essential not only for more detailed understanding of bacteriophage-host interactions [1, 2], but also for applied uses of prophage in phage therapy for bacterial infections [6,8] by the control of prophage gene expression.

Raman spectroscopy has been applied for characterization of bacteriophage by Thomas et al. [13, 14]. Laser tweezers Raman spectroscopy (LTRS) or Raman tweezers [15-17], has also been used to observe lysis of individual *Escherichia coli* cells in an optical trap caused by temperature induction of λ prophage and external lysozyme [18]. Raman spectroscopy has also been used to identify phage in cows' milk, where phage can negatively affect subsequent bacterial fermentations [19]. Although some Raman spectral and light scattering changes were observed in single-lysing cells in previous experiments [18], the heterogeneity in the dynamic changes in Raman spectra or cell length during prophage-induced lysis was not characterized for multiple individual cells in a population.

Here, we used Raman tweezers and live-cell phase contrast microscopy to characterize Raman spectral and cell length changes that occurred during the lysis of cells associated with individual *Bacillus subtilis* spores that carry the xylose-inducible defective PBSX prophage during spore germination, outgrowth, and vegetative growth. Raman tweezers was used to measure the time-lapsed Raman spectra of multiple individual cells incubated in various media with or without

addition of xylose that triggers the activation of the prophage. In addition, live-cell phase contrast microscopy was used to characterize the lengths of hundreds of individual cells incubated in nutrient-rich or nutrient-poor media with or without the addition of xylose, so that the lysis of many individual cells could be simultaneously recorded over up to 10 hours. We used *B. subtilis* spores that carry the PBSX prophage as the model system to study heterogeneity of prophage induction and lysis of individual cells among a population. The advantages of using the spore system include: i) bacterial spores are metabolically dormant, are very resistant to a variety of harsh conditions, and can survive for many years, and thus represent a convenient and relatively homogeneous starting point to generate cells in which prophage can be induced; and ii) spores can rapidly return to vegetative growth through germination followed by outgrowth, with germination triggered by specific nutrients and some non-nutrient agents [20, 21]. Thus, we may study both xylose-triggered prophage induction and spontaneous prophage induction during spore germination, outgrowth, and vegetative growth.

2. Materials and Methods

Bacterial strains, prophage and preparation of spores

The *B. subtilis* strains used in this work were MO012 that contains the defective prophage PBSX [9, 22, 23] and PS832 (wild-type). The PBSX late operon in the MO012 strain contains structural and lysin genes encoding proteins for making phage particles and host cell lysis [22, 23]. These genes are in a single operon controlled by the PL promoter, which is transcribed by RNA polymerase containing the Pcf sigma factor [9]. Upon germination and outgrowth, xylose induces expression of the Pcf sigma factor which promotes the induction of the prophage and associated lytic proteins (2 holins and 3 lysins) [23], resulting in the lysis of outgrowing spores or emergent

cells and presumably release of phage particles. The phage particle itself consists of a small head and long contractile tail packaged with ~13 kb of DNA exclusively from the host chromosome [22]. These phage particles are noninfectious since they do not contain a phage genome (hence they are considered defective phage) and are unable to infect phage-free bacteria [22]. Figure 1 shows the prophage life cycle and the monitoring of host cell length by live-cell microscopy.

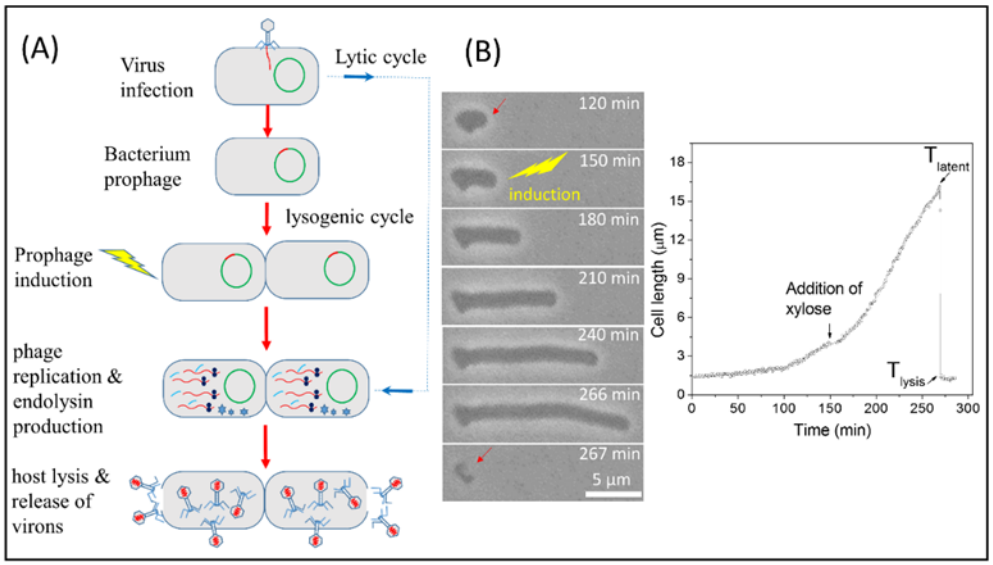

Figure 1. Prophage life cycle and host cell length observed by live-cell microscopy. (A) Phage infection of a host bacterium may result in a lytic cycle or a lysogenic state. In the latter the viral genome has integrated into the host DNA and is in a latent state in which the prophage is replicated with the bacterial chromosome. When the prophage is induced, viral replication and production of lysins begins via the lytic cycle, in which the virus commandeers the cell's macromolecular synthesis machinery. This leads to a host cell filled with new phage particles until the cell lyses and the phage are released. (B) Live-cell imaging with phase contrast microscopy was used to record the length of a cell derived from a MO012 spore after prophage induction. An outgrowing spore was induced with xylose at 150 min, with cell lysis at 267 min.

The rich growth medium used was L Broth (LB) medium (10 g/L tryptone, 10 g/L NaCl, 5 g/L yeast extract), supplemented with antibiotics [9]. Spores were prepared by nutrient exhaustion on 2xSG agar plates incubated for 5–7 days at 37°C, and then harvested by centrifugation, purified, and stored in water at 4 °C [20, 21]. Spores were free (>99%) of vegetative or sporulating cells, cell debris, and germinated spores, as observed by phase contrast microscopy.

Raman tweezers and live-cell phase contrast microscopy

The Raman tweezers system used in this work was described previously [17, 24]. Briefly, a laser beam at 780 nm is introduced into an inverted microscope (Nikon, TiS) that contains an external phase contrast system and an immersion objective (Plan Apo 60×, NA1.4) to form a single-beam optical trap. A spore or growing cell in an aqueous medium can be trapped ~10 μm above the bottom quartz coverslip. Backward Raman scattering light from the trapped cell exceited by the same laser was collected and focused on the entrance slit of a spectrograph (Princeton Instruments, LS-785) equipped with a back-illuminated deep depletion charge coupled device (Princeton Instruments, PIXIS 400BR).

The live-cell imaging of hundreds of individual cells was performed with phase contrast microscopy incorporated in Raman tweezers [17]. Phase contrast images were captured with a digital CCD camera (1,392 x1,040 pixels) at a rate of 1 frame per 15 s for up to 10 hours. A home-made auto-focus system was developed to actively lock in the focus of the objective, in which a diode laser at 650 nm was introduced to detect the distance change between the objective and the surface of the sample coverslip. The feedback electronic signal was added to a piezo attached on the objective to lock its position. The measured long-term stability of the focus locking along the z direction was ~10 nm.

Experimental procedures

The detailed information on (a) monitoring phage induction and lysis of MO012 cells with a microplate reader, (b) Raman measurement of kinetics of prophage induction in a cell population in LB medium, (c) monitoring prophage induction and cell lysis from an optically trapped single spore by Raman tweezers, and (d) spore germination, outgrowth and vegetative growth, and phage lysis on an agar pad monitored by live-cell imaging, can be found in the Supporting Information.

159 **Data analysis**

160 The Raman spectra were recorded in the "fingerprint" range from 500 to 1800 cm^{-1} with a spectral
161 resolution of ~6 cm^{-1}. The background spectrum was taken under the same acquisition conditions
162 without the cell in the trap and subtracted from the collected spectra of individual cells [16, 17].
163 The subtracted spectra were then smoothed and baseline-corrected using Spectragryph software,
164 and peak heights at particular wavenumbers were read out. In the time-lapsed measurements with
165 a population, the spectra of individual cells were normalized to a specific band at 1452 cm^{-1} that
166 had only a minimal change in peak intensity, in order to correct for variations among individual
167 cells. The image data of microscopy were processed and analyzed by a Matlab program to locate
168 and label individual spores and to calculate spore's phase contrast intensities by averaging the
169 pixel intensity of 40 by 40 pixels that covered each individual spore [24]. The lengths of individual
170 growing cells were extracted from the time-lapse phase contrast images with an accuracy of ~0.2
171 μm using ImageJ software and plotted as a function of incubation time. Movie clips were made
172 from the acquired phase contrast images using ImageJ software.
173
174 **3. Results**

175 **Growth of bacteria from spores and monitoring of prophage induction**

176 Using a multiplate reader allowed the monitoring of time-lapse values of OD_{600} (optical density at
177 600 nm) and growth curves of MO012 spores suspended in LB medium with and without xylose
178 (**Figure 2A**). Spore germination and growth in LB medium without xylose proceeded normally.
179 After the decrease in absorbance coinciding with spore germination, the absorbance of the
180 suspension began to increase during the period that coincides with spore outgrowth and then
181 vegetative growth (black curve in **Figure 2A**). Microscopy analysis of cells sampled after a 5 hour-

incubation without xylose is shown in **Figure 2B**. In the presence of xylose, spores appear to germinate normally with the same decrease in OD_{600} value as seen without xylose. However, microscopy analysis of cells after a 5 hour-incubation with xylose in LB medium, revealed the presence of empty spore coat remnants, as all spores had lysed (**Figure 2C**). Thus, the addition of xylose at t=0 h can induce the expression of PBSX-associated cell lysins, resulting in lysis of some outgrowing spores and growing cells.

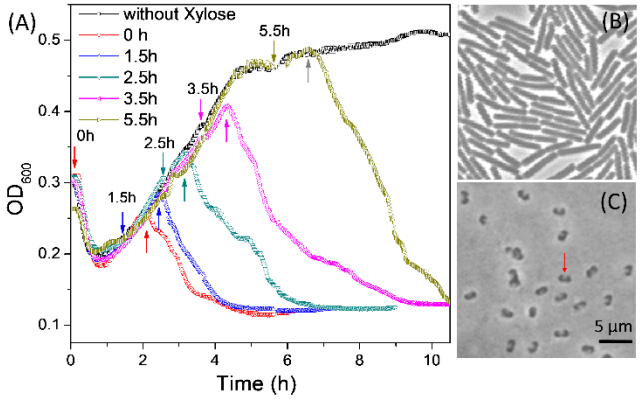

Figure 2. Growth and lysis of MO012 spores incubated in LB medium without or with xylose. (A) OD_{600} associated with the germination, outgrowth, and vegetative growth of MO012 spores at 37 °C without or with the addition of xylose to 1.25% at various times. The downward arrows show the time points at which the xylose was added and upward arrows show the time points at which cell lysis started. (B, C) Images of the cells after 5 hour-incubation in LB medium without xylose addition (B) and with the addition of xylose at t=0 h (C). The red arrow shows a spore coat remnant.

To test the effect of the growth stage on prophage induction, we added xylose at various times (t=1.5, 2.5, 3.5, and 5.5 h) to heat activated MO012 spores incubated in LB medium and recorded the time-lapsed OD_{600} values of the cultures. Notably, following the addition of xylose, the OD_{600} values continued to increase for a short period, presumably due to continued cell growth, and then declined to a lower level than the initial OD_{600}, corresponding to cell lysis. The time from the addition of xylose to the start of the OD_{600} decline is defined as the latent time (T_{latent}) for phage induced lysis, which was ~40 min when xylose was added at t=2.5 h, and 120 min when added at

t= 0 h. This suggests that the addition of xylose during exponential growth significantly reduces the latent time prior to phage induced lysis.

Time-lapse Raman spectra of spore populations incubated in LB medium with or without xylose

To determine the kinetic changes in molecular components inside the cells during germination, outgrowth, vegetative growth and cell lysis upon prophage induction, we measured time-lapse average Raman spectra of individual cells incubated in LB medium with or without xylose. Heat-activated spores were first incubated in LB medium at 37 °C in a shaking incubator for 2.5 hours, and then xylose was added to 1.25% to trigger prophage induction (**Figure 3A, B**) or no xylose was added (**Figure 3C, D**). Aliquots were removed from the cultures at different time points (t=5, 15, 30, 60, 90, 120, 150 and 180 min, respectively) after the addition of xylose, Raman spectra were measured from ~50 randomly chosen individual cells at each time point (labeled as t_5 to t_{180}), and the averaged spectra were processed by the subtraction of background spectra and baseline correction and normalized to the peak intensities of 1452 cm^{-1} band (Figure 3A, C). The relative peak intensities of 782, 1095, and 1452 cm^{-1} bands were calculated by dividing the values at time point t_5. In the culture with xylose addition, intensities of Raman bands at 782 cm^{-1} (C,U), 1095 cm^{-1} (OPO), 667, 723, 810, and 1572 cm^{-1} that are due to nucleic acids (**Table S1**) gradually decreased to zero (**Figure 3A, B**), while bands associated with other cellular components, including 1004 cm^{-1} (Phe), 1452 cm^{-1} (protein and lipids CH_2), 1659 cm^{-1} (protein amide I), as well as 643 cm^{-1} and 854 cm^{-1} (Tyr), 1209 cm^{-1} and 1609 cm^{-1} (Tyr and Phe) and 1251 cm^{-1} (protein amide III) were only slightly decreased. The disappearance of nucleic acid-associated Raman bands suggests the release of nucleic acids from the lysed cells. The presence of protein/lipid Raman bands at the later time points when most cells had lysed in the culture sample is likely

contributed by the lysed spores' coats (**Figure 2C**), which were captured by Raman tweezers. In contrast, in the culture without xylose (**Figure 3C, D**), the intensities of both the nucleic acid and protein/lipid bands were almost unchanged throughout the time course, consistent with the presence of intact cells.

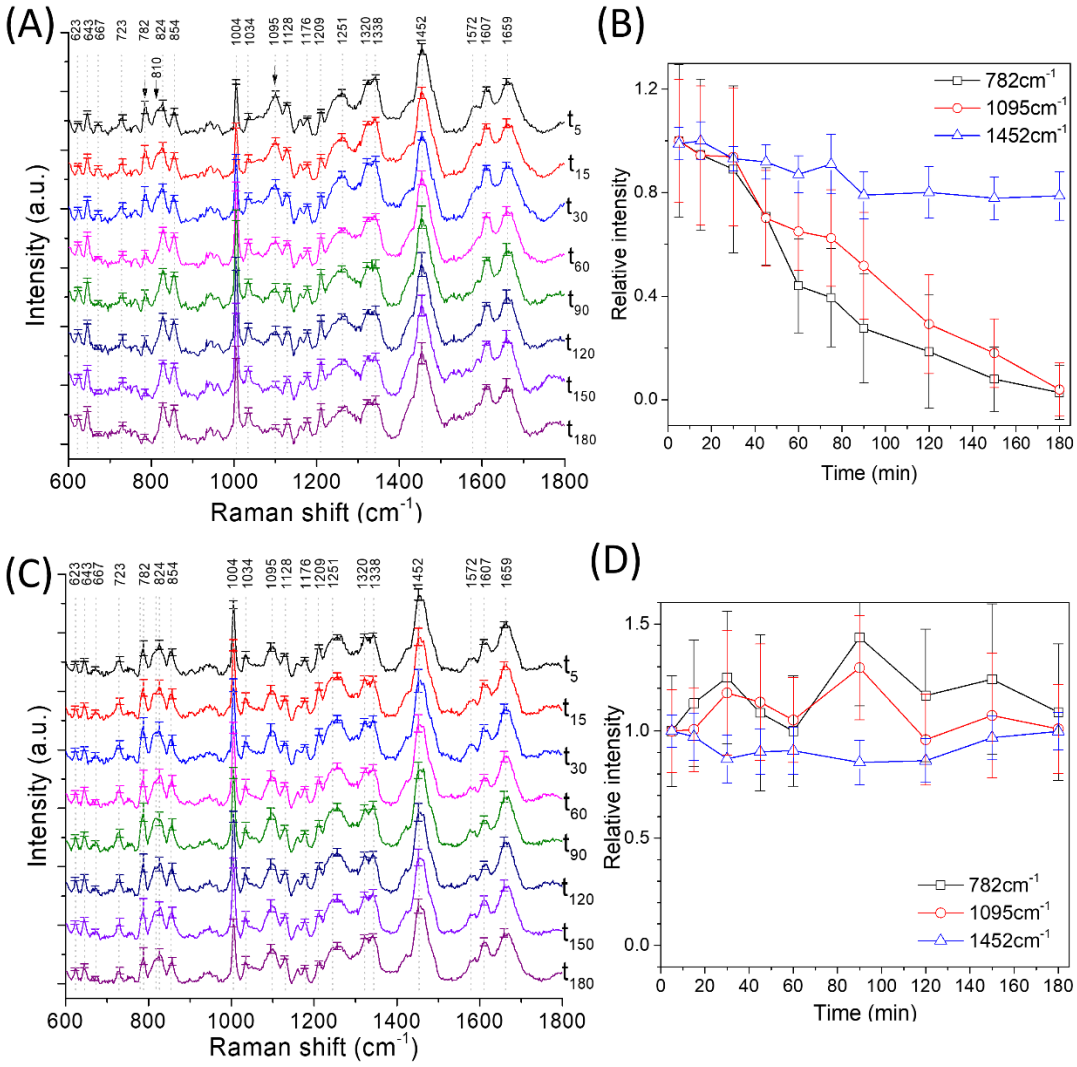

Figure 3. Time-lapse Raman spectra of MO012 spores incubated in LB medium with or without xylose. (A) Average Raman spectra of spores in LB medium with xylose and (B) relative intensities of various peaks as a function of the incubation time after the addition of xylose. The peak intensities were divided by the intensities at t_5 to obtain the relative intensities. (C) Average Raman spectra of spores in LB medium without xylose and (D) relative intensities of various peaks as a function of incubation time. Raman spectra of individual cells suspended in PBS at room temperature were measured with a laser power of 20 mW at 780 nm and an acquisition time of 30s. The error bars show the standard devivation among individual cells.

Time-lapse Raman spectra of a single optically trapped cell incubated in LB medium with xylose

To determine the dynamic changes of an individual cell during prophage induction and cell lysis, we measured time-lapse Raman spectra of a single trapped cell in LB medium with xylose. Heat-activated MO012 spores were first incubated in LB medium at 37 °C for 2.5 hours. Following addition of xylose, a growing cell was optically trapped and its Raman spectra were acquired sequentially with a low laser power to minimize photo-damage. Unlike the time-lapse spectra averaged over a cell population, following the addition of xylose, the intensity of the nucleic acids band at 782 cm^{-1} (C, U) of the trapped cell was nearly unchanged for ~99 min before a rapid drop, and the intensity at 1095 cm^{-1} (DNA OPO) band even increased ~20% before the rapid drop (**Figure 4B, C**). Accompanying the rapid drop in nucleic acid band intensities, the intensities of the protein/lipid bands at 1452 cm^{-1} and 1659 cm^{-1} (amide I) also exhibited a rapid decrease but not to zero, and there was a sudden change in the brightness of the phase contrast image of the lysing cell (Figure 4A), although the brightness of the phase contrast image for a growing cell was much lower than that for a dormant spore. The existence of the lag time prior to the rapid drop in nucleic acids and protein/lipid bands suggests that the cell continued to grow after the addition of xylose before rapid cell lysis. The lag time prior to cell lysis might vary among individual cells in a population so that the averaged Raman spectra of a cell population did not show a rapid decrease in nucleic acids band intensities at 782 cm^{-1} and 1095 cm^{-1} (Figure 3A, B). The larger decrease in protein/lipid bands of a single trapped growing cell than that of the cell population in Figure 3B, may be due to the shedding of the spore coat remnant from some trapped growing cells.

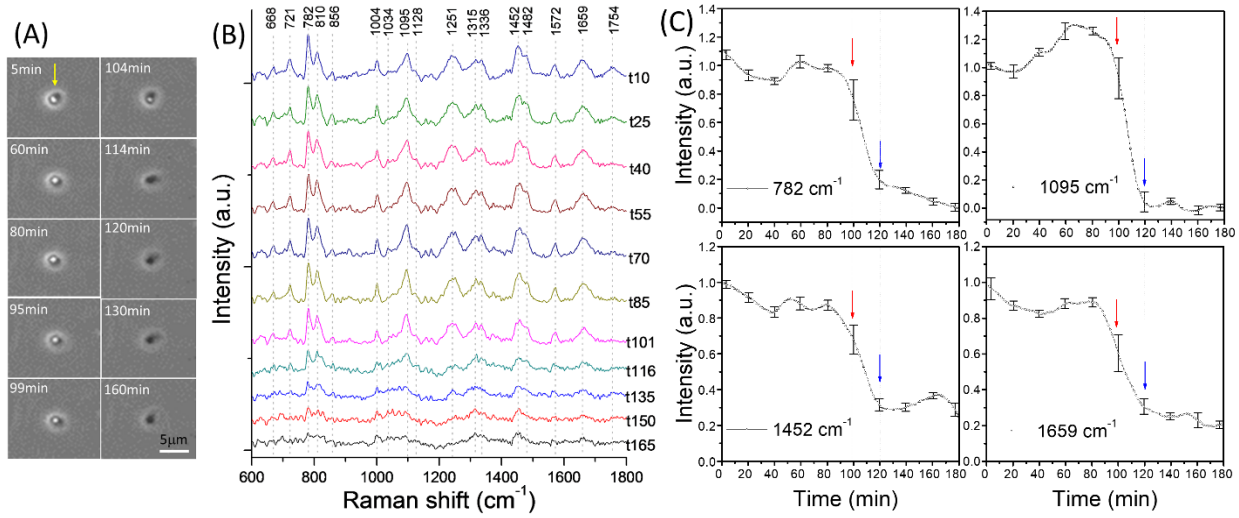

Figure 4. Time-lapse Raman spectra and phase contrast images of a single optically trapped MO012 cell incubated in LB medium with xylose addition to 1.25%. (A) Sequential images of the trapped cell. (B) Time-lapse Raman spectra of the trapped cell. The heat-activated MO012 spores were first incubated in liquid LB medium at 37 °C for 2.5 h. Following addition of xylose, a growing cell was optically trapped with a laser power of 3 mW at 780 nm and its Raman spectra were acquired sequentially with an acquisition time of 90 s. (C) The peak intensities of 782, 1095, 1455, and 1655 cm^{-1} bands as a function of incubation time after xylose addition. The error bars show the standard devivation among ten adjacent time points.

Heterogeneity in cell lysis of individual cells on LB agar with xylose

Figure 5A and B show live-cell phase contrast images of single MO012 spores incubated on LB agar with and without xylose. At the beginning, the spores were dormant, appearing bright under phase contrast microscopy. Within 1-2 hours, most spores had germinated and entered outgrowth, appearing as phase dark and somewhat swollen. Starting at 2.5-3 hours, the outgrown spores began rapid growth and some individual cells in xylose-containing medium began to lyse, with most cells completing lysis within 5 hours (**Figure 5A**, SI **Movie S1**). **Figure 5C** shows lengths of multiple individual outgrowing spores/cells as a function of the incubation time in xylose-containing medium. Surprisingly, single spores underwent a long latent period T_{latent} (228±41.4 min) for germination, outgrowth, and vegetative growth, followed by a short period of cell burst, ΔT_{burst}, in 1.5±0.8 min with an elongation length L_{latent} of 8.2±5.5 μm (SI **Table S2**). Apparently, the timing of lysis of individual cells by prophage induction in LB medium with xylose is highly heterogeneous (SI **Movie S1**), as indicated by widely varying latent times T_{latent}. As a comparison, spores incubated on LB agar without the addition of xylose germinated, outgrew and grew normally and did not show cell lysis (**Figure 5B** and **Figure 5D**). In addition, the presence of xylose in the medium did not affect the germination of MO012 spores in LB or L-valine medium (SI **Figure S1** and **Table S2**).

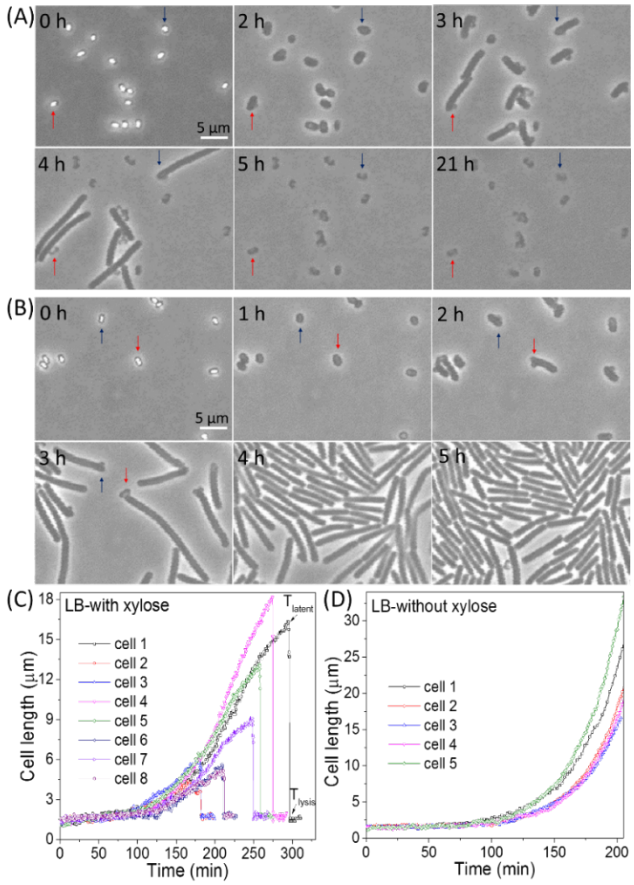

Figure 5. Live-cell imaging and cell lengths of single MO012 spores incubated on LB agar with and without xylose. Heat-activated MO012 spores were incubated at 37 °C on LB agar pads with or without the addition of xylose to 1.25% for ~21 hours. Time-lapse phase contrast images were acquired at a rate of 15s per frame for spores (A) with xylose and (B) without xylose. Cell lengths of multiple individual growing spores incubated in LB agar with (C) or without (D) xylose were extracted from the time-lapse images. The red and dark blue arrows show two germinating, growing, and lysing spores.

Figure S2 shows time-lapse images, cell lengths and normalized cell volumes of an individual spore incubated on LB agar with xylose. The kinetic curve of cell length as a function of incubation time can be characterized by a number of parameters: $T_{release}$ is the time at which the spore completes the release of its depot of Ca-DPA (dipicolinic acid in a 1:1 chelate with Ca^{2+}) in an early germination step [17, 24]; T_{cortex} is the time at which the spore completes lysis of its peptidoglycan cortex layer and enters into outgrowth (Figure S1B); T_{elong} is the time at which the outgrown spore initiates a rapid increase in cell length and volume and begins vegetative growth;

306 T_{latent} is the time at which the cell starts lysis with a cell length as L_{latent}; and T_{lysis} is the time at
307 which the cell competes lysis. The latent period is the period from the addition of xylose to activate
308 prophage induction (T_0) to T_{latent}, and the lysis period ΔT_{burst} is the difference between T_{lysis} and
309 T_{latent}.

310 In order to shorten the average latent time between the addition of xylose and the start of cell
311 lysis, we also incubated the spores on an LB agar pad without xylose for 2.5 hours to allow the
312 spores to proceed through germination and outgrowth, and then added the xylose to trigger
313 prophage induction (**Figure 1B**). As expected, the average latent time T_{latent} was reduced to
314 147±20.1 min with ΔT_{burst} of 1.0±0.4 min (**Table S2**), and the lysis of individual cells was also
315 highly heterogeneous among individuals in the population (**Figure S3** and **Movie S2**).
316
317 **Heterogeneous lysis of individual spores germinating on a L-alanine agar pads with xylose**
318 Incubation of *B. subtilis* spores in a medium of L-alanine alone leads to germination and outgrowth,
319 but would typically limit vegetative growth because of the minimal levels of some nutrients
320 required for optimal cell growth. **Figure S4** shows time-lapse images of MO012 spores incubated
321 on an L-alanine agar pad with or without xylose. Notably, individual spores on the L-alanine agar
322 pad with xylose went through germination and began outgrowth, and then suddenly lysed with a
323 heterogeneous latent time, without going into vegetative growth (**Figure S4A** and **Movie S3**).
324 **Figure 6** shows time-lapse images and cell lengths of two germinating, outgrowing, and lysing
325 spores on L-alanine agar with xylose. The average T_{latent} time was 342±41.4 min and ΔT_{burst} was
326 3.0±1.9 min (**Table S2**). The average cell length at T_{latent} was 2.3±0.4 μm, verifying the absence
327 of vegetative growth and cell division in L-alanine alone.

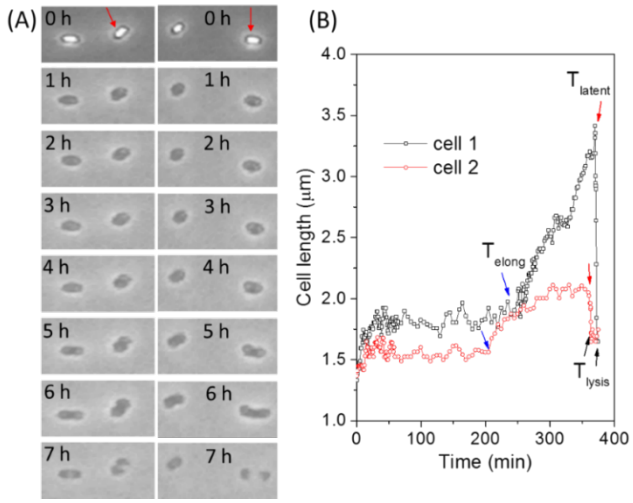

328

329 **Figure 6.** Time-lapse images (A) and cell lengths of two germinating, outgrowing, and lysing
330 MO012 spores on 10 mM L-alanine agar with 1.25% xylose at 37 °C. (B) Cell length of the two
331 individual spores versus incubation time..
332

333 **Spontaneous prophage induction and cell lysis of individual spores on minimal medium with**
334 **and without xylose**

335 Minimal medium is a nutrient-poor medium that limits the growth of *B. subtilis* cells [9]. **Figure**
336 **S5** shows time-lapse images of MO012 spores incubated on minimal medium agar with and
337 without xylose addition. It was found that the presence of xylose caused cell lysis after the spores
338 proceeded through germination and outgrowth (**Figure S5A**; **Table S2**). However, even cells
339 without xylose in the minimal medium exhibited cell lysis with a heterogeneous T_{latent} time
340 (282±51 min) and a L_{latent} value (4.1±2.2 μm) (**Figure S5B** and **Table S2**). **Figure S5C** shows cell
341 lengths of multiple individual MO012 spores incubated in minimal medium without xylose as a
342 function of the incubation time. This suggests that these growing cells underwent spontaneous
343 prophage induction in the minimal medium.

344

345 **4. Discussion**

346 In this work, we used Raman tweezers and live-cell phase contrast microscopy to characterize

Raman spectral and cell length changes during dynamic lysis of individual *B. subtilis* spores that carry PBSX prophage during germination, outgrowth, and vegetative growth. Several new findings were observed as follows.

First, the dynamics of lysis of individual cells induced by prophage was observed. The cell length curve recorded by live-cell microscopy provides a precise measure to characterize how long it takes for an individual cell to initiate cell lysis after prophage induction, something not available in studies with cell populations [1, 2], although time-lapse microscopy in microfluidic cultivation chambers allows the analysis of dynamic genetic circuits [25]. Lysis of *B. subtilis* MO012 cells from spores by prophage induction was observed in rich LB medium, poor L-alanine medium, and nutrient-limited minimal medium. In L-alanine alone and minimal medium with xylose, the spores went through germination and outgrowth, but the vast majority did not enter vegetative growth so that the cell lengths were not significantly increased by cell division prior to lysis (SI **Movie S3** and **Table S2**). Therefore, the subsequent events including the activation of the PBSX prophage-like genome, production of cell lysins and associated proteins, assembly of new phage particles, and the lysis of the host cell, can even occur inside an individual outgrowing spore. However, the precise mechanism determining the timing of these events is not fully understood [1, 2]. The factors affecting the period T_{latent} from the addition of the xylose that triggers prophage induction to cell lysis are unclear, but must include: (i) uptake of the xylose to a level sufficient to induce the PL promoter that activates the Pcf sigma factor, promoting the excision and activation of the PBSX prophage; and (ii) the synthesis of enough cell lysins sufficient to cause cell burst.

It is generally believed that exogenous molecules cannot readily penetrate into the dormant spore core [20, 21]. Indeed, analyses by Raman tweezers showed that certain exogenous molecules including nucleic acid stains and antibiotics are only taken into germinated spores soon after spores

370 release CaDPA at $T_{release}$ and reached maximal levels at T_{cortex} when germination is completed [26,
371 27]. Thus, it is likely that xylose uptake also starts when spores release their CaDPA and only
372 reaches maximal intraspore levels after germination is complete. However, the concentration of
373 xylose entering a single germinated spore might be much lower than that outside the spore,
374 although sufficient to trigger prophage induction. New virions made after prophage induction
375 reside within the host cell until it bursts due to lysin action [1, 2]. However, the precise number of
376 phage-derived lysins required to give cell lysis is unclear. The period from prophage induction to
377 the accumulation of a sufficient number of cell lysins might be between T_{elong} and T_{latent} in the
378 length curve of a single cell (**Figure 6B**) and varies from one cell to another in a population.
379 Second, and a rather surprising observation is that a whole growing cell chain containing 4-
380 8 cells often bursts simultaneously within a very short interval (~ 1 min) in LB medium with xylose
381 (**Figure 5B** and **Movie S1**). In a nutrient-rich medium with xylose, while the uptake of xylose
382 triggers prophage induction resulting in production of cell lysins and associated proteins, the host
383 cell starts vegetative growth at T_{elong} and initiates rapid cell division. In rapid growth, the host cell
384 seems to grow and divide normally, and the length of a single cell prior to lysis in LB medium is
385 8.2±5.5 μm with a latent time T_{latent} of 228±41.4 min, which is much shorter than the 342±41.4
386 min in L-alanine alone with xylose (with a cell length of 2.3±0.4 μm). The latent time T_{latent} can
387 be reduced to 147±20.1 min by adding xylose at 2.5 h after pre-incubation in LB medium, while
388 the cell length is 8.2±2.0 μm (SI **Table S2**). This indicates that the rate of prophage induction and
389 cell lysis is faster in rich medium than in poor medium. These data also suggest that expression of
390 the induced phage genes and production of cell lysins and associated proteins might occur during
391 rapid growth of the host cell in a rich medium. Presumably when cell lysins inside the cell
392 accumulate to a certain level, the host cell bursts. Notably, the host cell may actually be multiple

393 cells that have divided but not separated, and thus somehow the lysis of one cell in a chain results
394 in lysis of adjacent cells as well.

395 Third, the heterogeneity in lysis of individual cells among a population by prophage
396 induction is characterized by the heterogeneous latent time T_{latent}. This time for an individual spore
397 might be affected by several events, including $T_{release}$ at which the spore competes the release of
398 CaDPA, T_{cortex} at which the spore cortex lyses, T_{elong} at which the outgrowing spore starts rapid
399 vegetative growth, and uptake of xylose, expression of phage genes and production of cell lysins
400 and cell lysis at T_{latent}. The mechanism that determines the heterogeneity of these time points among
401 different individual spores or cells has yet to be determined. It was previously observed that $T_{release}$
402 and T_{cortex} are heterogeneous among individual germinating *Bacillus* spores [16, 20]. The variation
403 in the number of germination receptors possessed in individual spores is an major factor that affects
404 the duration of $T_{release}$ between the addition of germinant that triggers that activation of germination
405 receptors and CaDPA release, and an increase in the numbers of germinant receptors shortens
406 $T_{release}$ [21]. Similarly, the uptake of xylose might be heterogeneous among individual cells and a
407 fast xylose uptake in an individual cell would likely shorten T_{latent}. This is consistent with the
408 observation that the addition of xylose in vegetative growth after the completion of germination
409 and outgrowth, as the incubation in rich medium with xylose obviously shortens T_{latent} (**Table S2**).
410 Apparently, the uptake of xylose is much quicker in rich medium than that in poor medium, and is
411 faster in vegetative growth than that in germinated spore, due to the increase in metabolic capacity
412 in growing cells. This leads to a reduction in T_{latent} in growing cells.

413 Fourth, cell lysis by spontaneous prophage induction (SPI) was observed when MO012
414 spores were incubated in S7 minimal medium without xylose. In contrast, spontaneous prophage
415 induction was not observed in nutrient-rich LB medium and L-alanine alone without xylose. SPI

can be explained as the result of stochasticity in phage gene expression or the result of the spontaneous induction of the host SOS response [4, 5]. During growth, both extrinsic and intrinsic factors have an influence on the host genome and can lead to spontaneous DNA lesions or stalled replication forks, which leads to the expression of SOS genes to initiate cell growth inhibition and DNA repair or the inactivation of the phage repressor. Inactivation of phage repressors leads to depression of lysin genes' promoters which facilitates the excision of the prophage from the host genome [4]. However, the exact factors that effect SOS-dependent SPI of MO012 spores in minimal medium are unclear.

Finally, rapid decreases in nucleic acid bands at 782 and 1095 cm^{-1} and protein bands at 1452 and 1659 cm^{-1} of a single trapped cell observed by Raman spectroscopy coincide with cell lysis as observed by live-cell microscopy. Empty remnants of spore coat material and lysed spores accompany cell lysis (**Movie S1**), resulting in the release of nucleic acids and some proteins from the cell body, while the spore coat remains associated with the outgrowing spore. Therefore, nucleic acid bands exhibit a rapid drop to zero, but protein and lipid bands at 1452 and 1659 cm^{-1} are retained in the lysed spore.

Overall, the results of this study provide new insight into heterogeneity and dynamics of prophage-induced lysis of individual *Bacillus* spores during germination, outgrowth, and vegetative growth, demonstrating that Raman tweezers and live-cell phase contrast microscopy can collectively confer a route to enhanced resolution of analysis of individual cells undergoing phage-mediated lysis within a larger population.

ASSOCIATED CONTENT

Supporting Information

The Supporting Information is available free of charge online. It contains experimental procedures, supplementary movies, tables, and figures. **Table S1**: Raman bands and tentative assignments; **Table S2**: kinetic parameters for germination, outgrowth, and lysis of MO012 spores. **Movie S1**: MO012 spores incubated on a LB agar pad with xylose added at T_0; **Movie S2**: spores on a LB agar pad with the addition of xylose after 2.5 h incubation. **Movie S3**: spores incubated on an agar pad containing L-alanine.

Acknowledgments

This work (MW and YL) was supported by the National Natural Science Foundation of China (grants 91751110 and 61775036) and China Postdoctoral Science Foundation (2020M673554XB). MW and YL acknowledge the support from the BaGui scholar program of Guangxi Province, China.

References

1. Feiner, R.; Argov, T.; Rabinovich, L.; Sigal, N.; Borovok, I.; Herskovits, A. A new perspective on lysogeny: prophages as active regulatory switches of bacteria, Nat. Rev. Microbio. **2015**, 13 (10), 641–650.
2. Sausset, R.; Petit, M.A.; Gaboriau-Routhiau, V.; De Paepe, M. New insights into intestinal phages. Mucosal Immunol. **2020**, 13, 205 – 215.
3. Canchaya, C.; Proux, C.; Fournous, G.; Bruttin, A.; Brüssow, H. Prophage genomics. Microbiol. Mol. Biol. Rev. **2003**, 67, 238–276.
4. Nanda, A.M.; Thormann, K.; Frunzke, J. Impact of spontaneous prophage induction on the fitness of bacterial populations and host-microbe interactions. J. Bacteriol. **2015**, 197, 410-419.
5. Alexeeva, S.; Martínez, J.A.; Spus, M.; Smid, E.J. Spontaneously induced prophages are abundant in a naturally evolved bacterial starter culture and deliver competitive advantage to the host. BMC Microbiol. **2018**, 18, 120.
6. Dedrick, R.M.; Guerrero-Bustamante, C.A.; Garlena, R.A.; Russell, D.A.; Ford, K.; Harris, K.; Gilmour, K.C.; Soothill, J.; Jacobs-Sera, D.; Schooley, R.T.; Hatfull, G.F.; Spencer, H. Engineered bacteriophages for treatment of a patient with a disseminated drug-resistant *Mycobacterium abscessus*. Nat. Med. **2019**, 25, 730–733.
7. Lu, T. K.; Koeris, M. S. The next generation of bacteriophage therapy. Curr. Opin. Microbiol. **2011**, 14, 524–531.
8. Boling, L.; Cuevas, D.A.; Grasis, J.A.; Kang, H.S.; Knowles, B.; Levi, K.; Maughan, H.; McNair, K.; Rojas, M.I.; Sanchez, S.E.; Smurthwaite, C.; Rohwer, F. Dietary prophage inducers and antimicrobials: toward landscaping the human gut microbiome. Gut Microbes **2020**, 11, 721-734.

9. Mohamed, M.; Christie, G. A system for the expression and release of heterologous proteins from the core of *Bacillus subtilis* spores. FEMS Microbiol. Lett. **2018**, 365(23).
10. Choonara, B.F.; Choonara, Y.E.; Kumar, P.; Bijukumar, D.; Toit, L.C.; Pillay, V. A review of advanced oral drug delivery technologies facilitating the protection and absorption of protein and peptide molecules. Biotechnol. Adv. **2014**, 32, 1269-1282.
11. Reyes, A.; Haynes, M.; Hanson, N.; Angly, F.E.; Heath, A.C.; Rohwer, F.; Gordon, J.I. Viruses in the faecal microbiota of monozygotic twins and their mothers. Nature **2010**, 466, 334–338.
12. Willner, D.; Furlan, M.; Schmieder, R.; Grasis, J.A.; Pride, D.T.; Relman, D.A.; Angly, F.E.; McDole, T.; Mariella, R.P.; Rohwer, F.; Haynes M. Metagenomic detection of phage-encoded platelet-binding factors in the human oral cavity. Proc Natl Acad Sci. **2011**, 108, 4547–4553.
13. Incardona, N.L.; Prescott, B.; Sargent, D.; Lamba, O.P.; Thomas, G.J. Phage phiX174 probed by laser Raman spectroscopy: evidence for capsid-imposed constraint on DNA secondary structure. Biochemistry (Mosc.) **1987**, 26, 1532–1538.
14. Aubrey, K.L.; Casjens, S.R.; Thomas, G.J. Secondary structure and interactions of the packaged dsDNA genome of bacteriophage P22 investigated by Raman difference spectroscopy. Biochemistry (Mosc.) **1992**, 31, 11835–11842.
15. Xie, C.A.; Dinno, M.A.; Li, Y.Q. Near-infrared Raman spectroscopy of single optically trapped biological cells. Opt. Lett. **2002**, 27, 249-251.
16. Chen, D.; Huang, S.S.; Li, Y.Q. Real-time detection of kinetic germination and heterogeneity of single Bacillus spores by laser tweezers Raman spectroscopy. Anal. Chem. **2006**, 78, 2936-6941.
17. Kong, L.; Zhang, P.F.; Wang, G.W.; Setlow, P.; Li, Y.Q. Characterization of bacterial spore germination using phase-contrast and fluorescence microscopy. Raman spectroscopy and

optical tweezers. Nat. Protocols **2011**, 6, 625.

18. Chen, D.; Shelenkova, L.; Li, Y.Q.; Kempf, C. R.; Sabelnikov, A. Laser tweezers Raman spectroscopy potential for studies of complex dynamic cellular processes: single cell bacterial lysis. Anal. Chem. **2009**, 81, 3227–3238.
19. Acar-Soykut, E.; Tayyarcan, E. K.; Boyaci, I. H. A simple and fast method for discrimination of phage and antibiotic contaminants in raw milk by using Raman spectroscopy. J. Food Sci. Technol. **2017**, 55, 82–89.
20. Setlow, P.; Wang, S.W.; Li, Y.-Q. Germination of spores of the orders *Bacillales* and *Clostridiales*. Annu. Rev. Microbiol. **2017**, 71, 459–77.
21. Setlow P. The germination of spores of *Bacillus* species: what we know and don't know. J. Bacteriol. **2014**, 196, 1297–305.
22. Krogh, S.; Jørgensen, S.T.; Devine, K.M. Lysis genes of the *Bacillus subtilis* defective prophage PBSX. J. Bacteriol. **1998**, 180, 2110–7.
23. Freitag-Pohl, S.; Jasilionis, A.; Håkansson, M.; Svensson, L.A.; Kovačič R.; Welin M.; Watzlawick H.; Wang L.; Altenbuchner J.; Płotka M.; Kaczorowska A. K.; Kaczor-owski T.; Karlsson E. N.; Al-Karadaghi S.; Walse B.; Pohl, E. Crystal structures of the *Bacillus subtilis* prophage lytic cassette proteins XepA and YomS. Acta Crystallogr. D. Struct. Biol. **2019**, 75, 1028–1039.
24. Kong, L.; Zhang, P.; Setlow, P.; Li, Y. Q. Characterization of bacterial spore germination using integrated phase contrast microscopy, Raman spectroscopy, and optical tweezers. Anal. Chem. **2010**, 82, 3840–3847.
25. Locke, J.C.W.; Elowitz, M.B. Using movies to analyse gene circuit dynamics in single cells. Nat. Rev. Microbiol. **2009**, 7:383–392.

522 26. Kong, L.B.; Zhang, P.F.; Yu, J.; Setlow, P.; Li, Y.Q. Monitoring the kinetics of uptake of a
523 nucleic acid stain during the germination of single spores of *Bacillus* species. Anal. Chem.
524 **2010**, 82, 8717–8724.
525 27. Wang, S.W.; Setlow, B.; Setlow, P.; Li, Y.Q. Uptake and levels of the antibiotic berberine in
526 individual dormant and germinating *Clostridium difficile* and *Bacillus cereus* spores as
527 measured by laser tweezers Raman spectroscopy. J. Antimicrob. Chemoth. **2016**, 71(6), 1540-
528 1546.
529

Table of Contents Graphics